Supercapacitors based on low-temperature partially exfoliated and reduced graphite oxide

Jian Ye [a], Haiyan Zhang [a,*], Yiming Chen [a], Zhengdong Cheng [a,b], Li Hu [a], Qiyan Ran [a]

[a] Faculty of Materials and Energy, Guangdong University of Technology, Guangzhou 510006, China
[b] Artie McFerrin Department of Chemical Engineering, Texas A&M University, College Station, TX 77843, USA

ABSTRACT

Thermally exfoliated graphite oxide (GO) has been prepared at a low temperature and ambient pressure usually contains flourish oxygen functional groups. We find that complete oxidized graphite can be successfully expanded, as well as partially exfoliated and reduced at a very low temperature about 200 °C and ambient pressure without any supplementary conditions such as high vacuum or under hydrogen environment. The electrochemical properties of supercapacitor electrodes are studied by cyclic voltammetry (CV) and galvanostatic charge/discharge (DC) methods. Supercapacitors are constructed with as-prepared functionalized graphene have good electrochemical performance, with a maximum specific capacitance of 315 F g^{-1} at the charge/discharge current density of 100 mA g^{-1} using 1 M KOH electrolyte and a high charge/discharge efficiency of about 97%.

© 2012 Elsevier B.V. All rights reserved.

1. Introduction

Graphene has attracted great interest due to its special structure and unique electrical performance. Monolayer graphene was first prepared in 2004 by microcleaving highly ordered pyrolytic graphite (HOPG) by Andre Geim and Konstantin Novoselov at University of Manchester in England [1]. Afterwards, the high performance of graphene in electrics, optics, and mechanics has been explored with vast application prospect. At present, many physicists, material scientists and chemists are actively researching the applications of graphene. As a one-atom-thick two-dimensional (2D) crystal, Monolayer graphene can be wrapped up into zero-dimensional (0D) fullerenes and rolled into one-dimensional (1D) carbon nanotubes or stacked layer-by-layer into three-dimensional (3D) graphite [2–4]. At room temperature, thermal conductivity and carrier mobility of graphene are up to 5300 W m^{-1} K^{-1} [5] and 200,000 cm^2 V^{-1} s^{-1} [6], respectively. The Hall effect [7,8], high mechanical strength [9], high electron mobility [10] etc. are also exhibited in graphene at room temperature. In addition, graphene possesses ultrahigh specific surface area due to its unique 2D structure. The theoretical specific surface area of single-layer graphene is as high as 2600 m^2 g^{-1} [11].

Therefore, graphene has great potential applications in lithium ion batteries and supercapacitors.

So far, there are many studies on graphene synthesis and use of graphene in supercapacitors. At present, preparing graphene by chemical reduction of GO has been widely known. Sasha Stankovich et al. [12] synthesized graphene via chemical reduction of exfoliated graphene oxide. They found that GO was thermally unstable and started to lose mass upon heating blow 100 °C, the major mass loss occurred at 200 °C. Meryl D. Stoller et al. [13] prepared the chemically modified graphene by reducing GO with hydrazine, and the electrodes of as-prepared graphene had good electrochemical properties. The specific capacitance values were 135 F g^{-1}, 94 F g^{-1} and 99 F g^{-1} at a discharge current of 10 mA g^{-1} in 5.5 M KOH, TEABF$_4$/PC and TEABF$_4$/AN electrolytes, respectively. Yao Chen et al. [14] synthesized partially reduced graphene oxide by chemical reduction of GO with a weak reductant HBr. They retained fractional oxygen functional groups, 2-3 layers of graphene could be observed. The maximum specific capacitance of the graphene electrodes was 348 F g^{-1} and 158 F g^{-1} in 1 M H$_2$SO$_4$ and BMIPF$_6$, respectively. Otherwise, Oxidation and thermal exfoliation of graphite provides an efficient way for preparing graphene but usually needs high temperature or rapid heating. Hannes C. Schniepp et al. [15] successfully prepared functionalized single graphene sheets via rapidly heating the complete oxidized graphite to 1050 °C (heating rate > 2000 °C min^{-1}) under argon

* Corresponding author. Tel.: +86 020 39323232; fax: +86 020 39322572.
 E-mail address: hyzhang@gdut.edu.cn (H. Zhang).

environment. Michael J. McAllister et al. [16] prepared graphene by directly putting the GO into a furnace that preheated to 1050 °C. They suggested that exfoliation occurred when the pressure produced by decomposition of oxygen functional groups was high enough to overcome the van der Waals forces between the graphene layers and a critical temperature of 550 °C must be exceeded. S. Vivekchand et al. [17] prepared graphene by three different methods. The samples prepared by exfoliating GO at high temperature (1050 °C) exhibited the highest specific capacitance in 1 M H_2SO_4, up to 117 F g^{-1}. Furthermore, as a convenient and rapid heating sources, microwave irradiation has been applied in exfoliating GO. Yanwu Zhu et al. [18] reported a simple and versatile method to achieve the exfoliation and reduction of GO simultaneously by irradiating GO in a microwave oven and the specific capacitance of 191 F g^{-1} was obtained in 5 M KOH aqueous solution.

Recently, there are several studies on synthesizing graphene by exfoliating GO at a very low temperature with some supplementary conditions. Adarsh Kaniyoor et al. [19] prepared graphene via hydrogen induced reduction–exfoliation of GO at a low temperature (200 °C). They suggested that hydrogen might react with −OH groups in GO that supplied enough energy to cause the disruption and exfoliation. Wei Lv et al. [20] also produced graphene at a low temperature (200 °C) and must be accompanied with a high vacuum environment. The high vacuum which introduced a negative pressure surrounding the graphene layers could exert an outward drawing force on the expanding graphene layers. Thermogravimetric differential scanning calorimetry revealed that most oxygen-containing functional groups were removed at a narrow temperature range (150 °C–250 °C). The specific capacitance values of the graphene were 264 F g^{-1}, 122 F g^{-1} with the current density of 100 mA g^{-1} in KOH, $MeTt_3NBF_4$ (AN) electrolytes, respectively.

Currently, there are few reports on GO expansion at 200 °C and ambient pressure without any supplementary conditions such as high vacuum or under hydrogen environment. In this work, we report the supercapacitors with high specific capacitance based on functionalized graphene materials prepared by exfoliating GO at 200 °C and ambient pressure without any supplementary conditions.

2. Experimental

2.1. Preparation of functionalized graphene

Completely oxidized graphite was prepared by a modified Hummers method [21]. Firstly, 92 ml concentrated H_2SO_4 (98 wt%) was added to a 500 ml conical flask which placed in an incubator set at a low temperature of 2 °C, the natural graphite powders (4 g) mixed with $NaNO_3$ (2 g) was added. The potassium permanganate (12 g) was added slowly, and stirring for 2 h, then the conical flask was put into a water bath of 35 °C, stirring for 2 h. After 184 ml deionized water was slowly added to the mixture solution, the temperature was risen to about 75 °C when keep stirring for a while. A suitable amount of hydrogen peroxide was added to turn the color of the solution into yellow. The mixture was filtered and washed using 5% HCl and deionized water until no sulfate ions filtrate detected, the solid was dried at vacuum oven for 24 h.

Functionalized graphene was obtained by thermal expansion of GO in an incubator at 200 °C for about 10 min. A large volume expansion was observed even accompanied with flame.

2.2. Characterization of functionalized graphene and measurement of electrochemical performance

X-ray diffraction (XRD; DMAX-Ultima IV, Rigaku Corporation, Japan) was employed to identify the degree of exfoliation of GO.
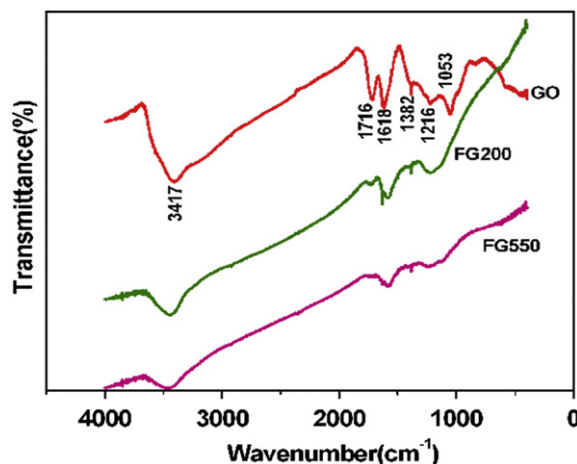

Fig. 1. FTIR spectra of GO, FG200, and FG550.

The surface morphology and crystal structure were observed by scanning electron microscopy (SEM; S3400N, Hitachi, Japan) and transmission electron microscopy (TEM; JEM-2010HR, Jeol, Japan). The surface chemical composition and chemical bonds were characterized by Fourier transform infrared (FTIR; Nicolet 380, Nicolet, USA) spectrometer. The defect and molecular vibration mode were measured by Raman spectra (Renishaw 2000 Confocal Raman Microprobe; Renishaw Instruments, England). The supercapacitor electrodes were prepared by as-prepared graphene, acetylene black, and polytetrafluoroethylene at a weight ratio of 8:1:1 homogenously spread well on foam Ni and dried at 60 °C at vacuum oven for 48 h, then pressed and cut it into a 16.2-mm-diameter wafer. Finally it was packed into button cell supercapacitors with 1 M KOH as electrolyte. The properties of packaged button cell supercapacitors were investigated by CV and DC measurements. CV curves were tested using an electrochemical work station (CHI660C; CH Instruments, Shanghai Chenhua Instrument Corporation, China). When scanning the potential from 0 to 0.8 V, the scan rates were 1, 5 and 10 mV s^{-1}, respectively. The DC and cycle life were tested by a battery testing system (CT2001A, Wuhan LAND Corporation, China), the current densities of charge/discharge varied from 100 to 400 mA g^{-1}.

3. Results and discussion

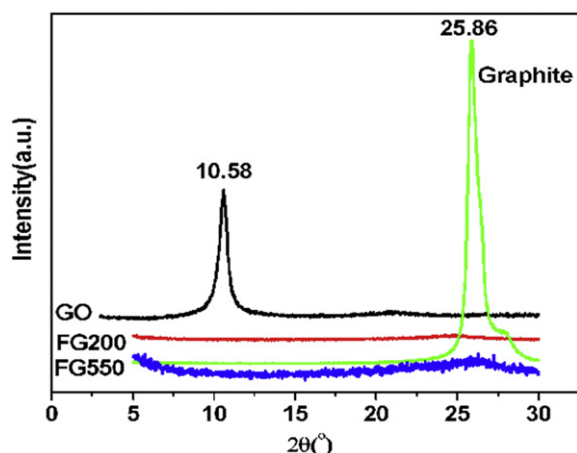GO was prepared from natural graphite when reacting with concentrated sulfuric acid and potassium permanganate. In the

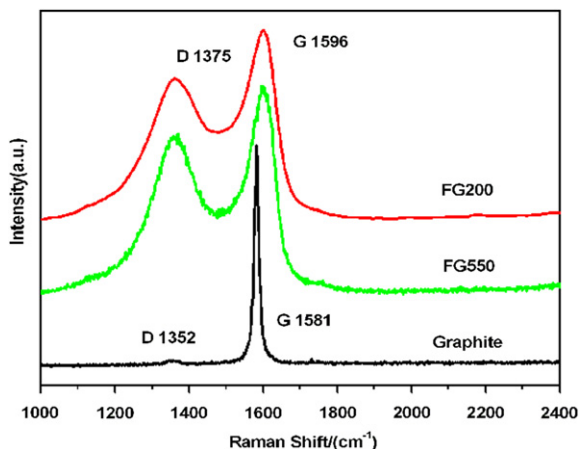**Fig. 2.** XRD patterns of graphite, GO, FG200, and FG550.

Fig. 3. Raman spectra of graphite, FG200, and FG550.

oxidation process, some carbon bonds were destroyed, the attraction between carbon layers was weakened. The interlayer was inserted with groups of hydroxyl, carboxy and epoxide. Fig. 1 shows the FTIR spectra of GO, FG200 (GO exfoliated at 200 °C), FG550 (GO exfoliated at 550 °C). The broad and intense peak at 3417 cm^{-1} was due to −OH. Owing to the stretching vibration of C═O on carboxy and water molecules, two obvious peaks showed up at 1716 cm^{-1} and 1618 cm^{-1}, respectively. The conspicuous peaks at 1382 cm^{-1}, 1216 cm^{-1} might be due to C−O, −OH of −COOH groups [19]. The peak at 1053 cm^{-1} was the vibration adsorption peak of C−O−C. Compared with GO, the intensity of FG200 adsorption peaks obviously decreased, but some adsorption peaks remained fairly strong such as those at 3417 cm^{-1}, 1618 cm^{-1}, 1382 cm^{-1}, 1216 cm^{-1}, where some oxygen functional groups existed, the oxygen groups just decomposed partially. The adsorption peak at 3417 cm^{-1} was further weakened and the peaks at 1716 cm^{-1}, 1382 cm^{-1}, 1216 cm^{-1} and 1053 cm^{-1} were almost disappeared in FG550 indicating that most functional groups were removed at 550 °C.

Fig. 2 shows the XRD patterns of natural graphite, GO, FG200, and FG550. The single intense diffraction peak in graphite and GO
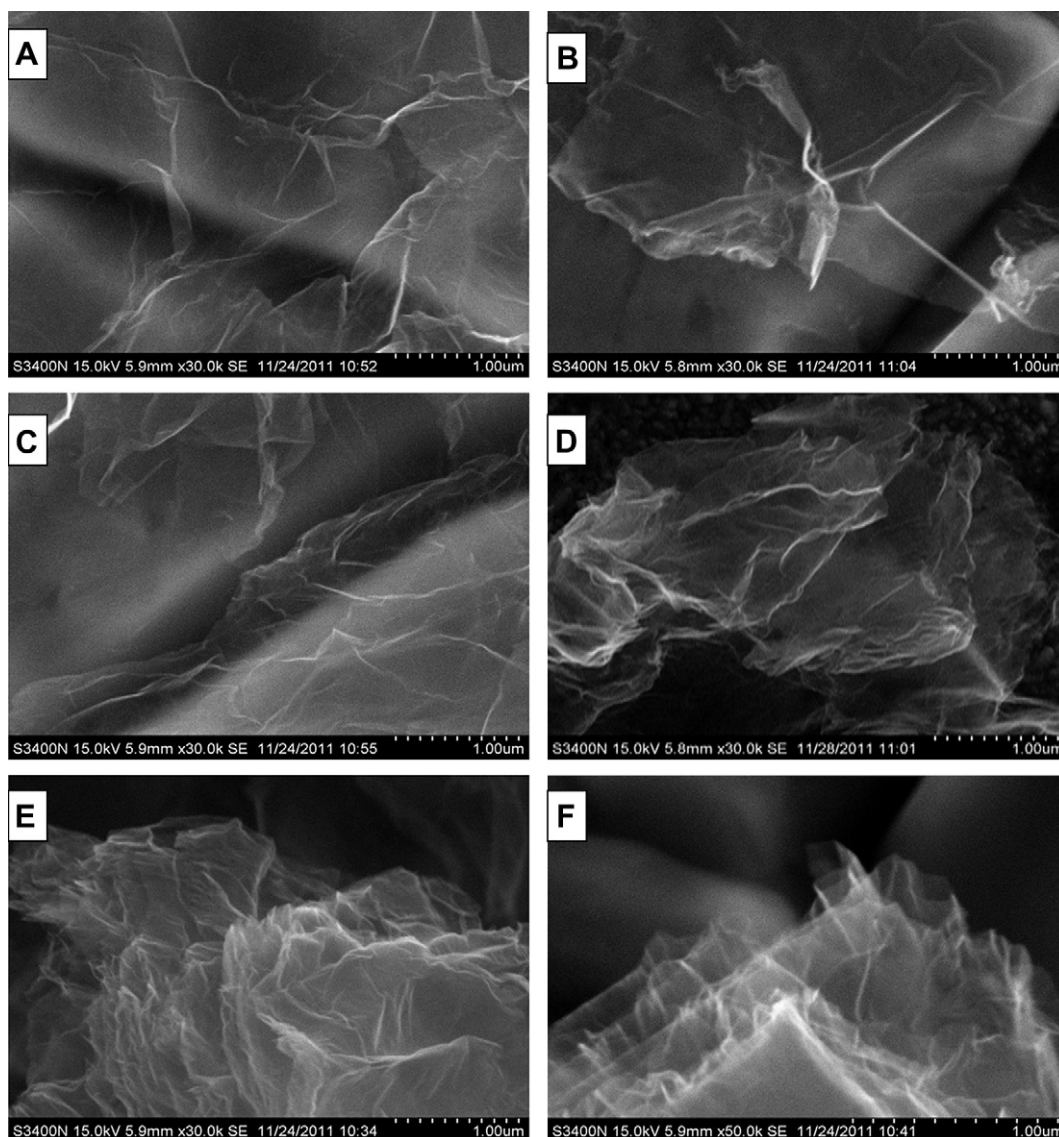

Fig. 4. SEM images of FG200: (A−C) The crumpled and transparent morphology; (D−F) A multi-layer "paper-like" structure.

were at 25.86° and 10.58°, respectively, indicating that graphite had been fully oxidized. The feature diffraction peak at 10.58° disappeared completely, a very weak diffraction peak emerged at 25° in FG200, FG550 sample, which was close to the feature peak of graphite, indicating exfoliation of GO and amorphous structures of as-prepared graphene.

Fig. 3 shows the Raman spectra of natural graphite, FG200, and FG550. Natural graphite had two Raman bands, the G band at 1581 cm^{-1} and a very weak D band at 1352 cm^{-1}, with the G band corresponded to the first-order scattering of E_{2g} mode and the D band corresponded to graphite edges [22–23]. From the Raman spectra, we clearly observed that both FG200 and FG550 contained two strong peaks, the G band at about 1596 cm^{-1} and D band at about 1357 cm^{-1}. The G band was close to that of the natural graphite. Due to the disorder vibration of carbon bond and defects, the intensity of D band increased dramatically and G band was broaden. Compared to natural graphite, the ratio of intensities of D and G band (I_D/I_G) was dramatically increased, predicting much defects and high disorder in both samples [24]. It was mainly attributed to oxygen-containing defects which caused by fiercely oxidation, as well as vacancies and topological defects caused by the release of carbon dioxide etc. during decomposition [25].

The SEM images in Fig. 4, A–C show that FG200 had a crumpled and transparent morphology. In Fig. 4, D–F, the graphene layers could stack together displaying a multi-layer "paper-like" structure where nanoscale pores generated. So the ions of electrolyte could easily get access to the gaps between the layers which contributed to electrochemical performance. The oxygen functional groups on the GO layers only partially decomposed at such a low temperature, the pressure generated by decomposition of oxygen functional groups might not high enough to overcome the Van der Waals forces could result in the stacked graphene layers [16,20].

Fig. 5 presents transmission electron microscopy (TEM) images of FG200. We observed that FG200 were winkled transparent flakes under low-magnification TEM in Fig. 5, A and B. High magnification TEM images showed that FG200 was crippling multi-layer structured. The number of the layers in Fig. 5C could be identified as 5–6, and the interlayer spacing was around 0.38 nm which just a little larger than the carbon interlayer space in graphite (0.34 nm) [12] indicated that the reduction of GO to a large extent and there was still a certain amount of oxygen-containing functional groups between layers might lead to a larger interlayer distance comparing to graphite. The weak and dispersing electron diffraction in Fig. 5D indicated that the FG200 did not have long range order [16].

We used the FG200 (Fig. 6A) and FG550 (Fig. 6B) as the supercapacitor electrodes and 1 M KOH as electrolyte. The properties of supercapacitors were investigated using CV and DC methods. Fig. 6 shows the CV curves of the supercapacitors, the shapes of all the CV curves were close to rectangular, but not full symmetrical, indicating a relatively excellent supercapacitive performance. The asymmetry was mostly caused by the fast and reversible redox reactions between the electrolyte and surface functional groups on graphene layers such as the transition of oxygen-containing groups of C=O groups and C–O groups. For example, unsaturated carbon atom might be combined with free oxygen to form carbonyl groups (C=O) and then carbonyl might be combined with H$^+$, OH$^-$ and free oxygen in the electrolyte to form –C–OH etc. [26].

The specific capacitance of the supercapacitor electrodes can be calculated through Eq. (1):

$$C_{sp} = \frac{dq}{m \cdot dV} = \frac{dq/dt}{m \cdot (dV/dt)} = \frac{i}{m \cdot (dV/dt)} \tag{1}$$

Where, C_{sp} is specific capacitance of the electrodes, dV/dt is scan rate of the potential, i is the current and m is the mass of
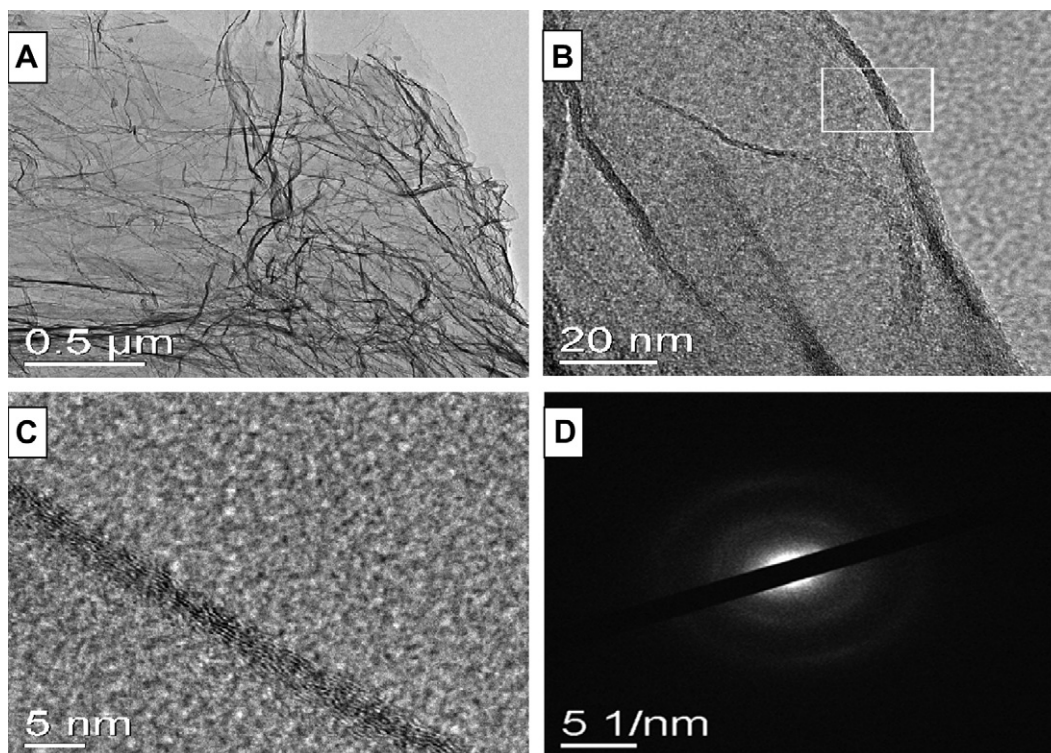

Fig. 5. TEM observations and electron diffraction image of FG200: (A, B) TEM images of low-magnification; (C) TEM image of high magnification of a part of FG200 in panel b; (D) Electron diffraction of the selection part in panel b.
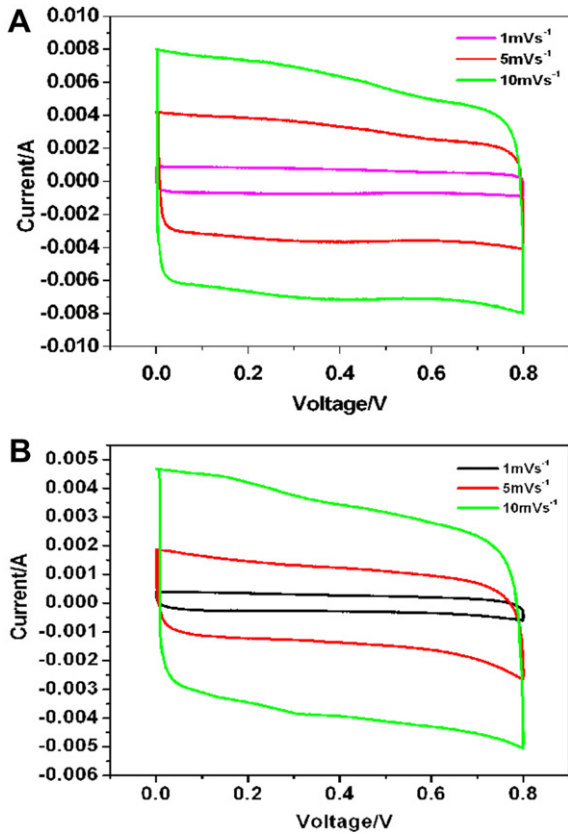
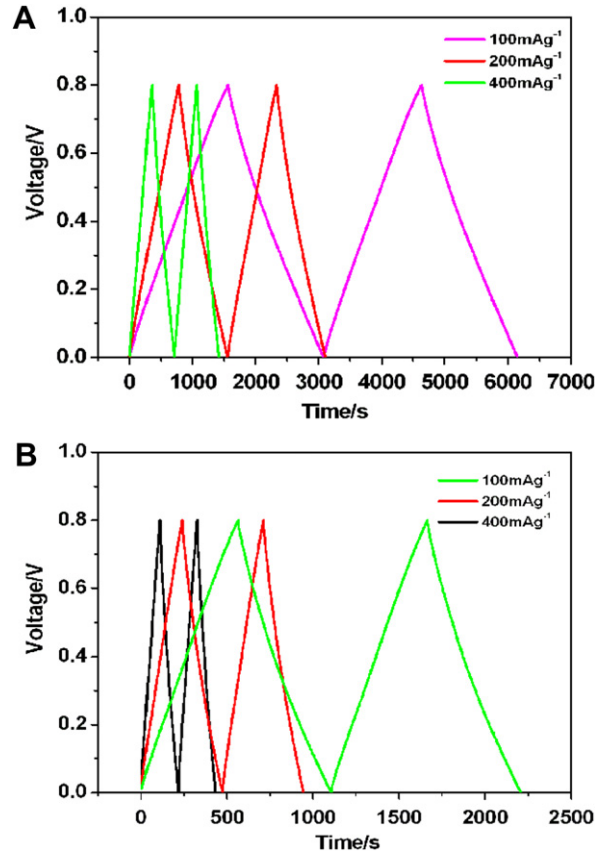**Fig. 6.** CV curves of supercapacitors based on FG200 (A) and FG550 (B) at different scan rates.

Fig. 7. Charge/discharge curves of supercapacitors based on FG200 (A) and FG550 (B) at different current densities.

the active materials of the electrodes. The obtained values are shown in Table 1.

As can be seen from Table 1, the specific capacitance of FG200 electrode reached 287 F g^{-1} at 1 mV s^{-1}. However, the specific capacitance of FG550 electrode had much lower specific capacitance of only about 128 F g^{-1}. As the scan rate increased, the specific capacitance of FG200 and FG550 decreased accordingly. The main reason was because when the scan rate increased, the ions in the electrolyte might not have enough time to enter into the complex micropores of electrodes leading to the high surface areas of graphene couldn't be fully utilized.

Fig. 7 shows the DC curves of FG200 (Fig. 7A) and FG550 (Fig. 7B) electrodes. The curves were almost isosceles triangles indicating typical electric double layer capacitance properties.

In this situation, we can calculate the specific capacitances of the electrodes through the following Eq. (2):

$$C_{sp} = \frac{\Delta q}{m \cdot \Delta U} = \frac{\Delta q}{m \cdot \Delta t} \cdot \frac{\Delta t}{\Delta U} = \frac{I \cdot \Delta t}{m \cdot \Delta U} \tag{2}$$

Where, m is again the mass of the active materials in electrodes, I is the discharge current density, ΔU is the potential variation value, Δt is the time corresponding to ΔU during the discharge process.

Because the supercapacitors were made by two symmetric electrodes, the specific capacitances of the supercapacitor electrodes should be doubled. The value results are shown in the following Table 2.

As can be seen from Table 2, when the current density of discharge was 100 mA g^{-1}, the specific capacitance value of FG200 reached the highest, up to 315 F g^{-1}. Compared to thermally exfoliated GO prepared at high temperature [17], the value had an increase of almost 200 F g^{-1} and slightly higher than low temperature (200 °C) expansion under high vacuum [20]. The main reason might be the oxygen-containing functional groups in GO could not be completely removed at such a low temperature and ambient pressure. The residual functional groups facilitated the penetration of aqueous electrolytes and introduced pseudocapacitive effects that contributed to the specific capacitance [14]. When the charge/discharge current density increased to 400 mA g^{-1}, the specific capacitance still kept a high value with only a slight decrease of 9%, indicating an excellent charge/discharge performance. Compared with FG200, the specific capacitance values of FG550 were far smaller. The main reason was because oxygen-containing groups in GO could be further decomposed at higher temperature (550 °C),

Table 1
Specific capacitances of electrodes at different scan rates.

Sample	Maximum specific capacitance/(F g^{-1})		
	1 mV s^{-1}	5 mV s^{-1}	10 mV s^{-1}
FG200	287 ± 5	246 ± 5	242 ± 5
FG550	128 ± 5	111 ± 5	104 ± 5

Table 2
Specific capacitances of electrodes at different current densities.

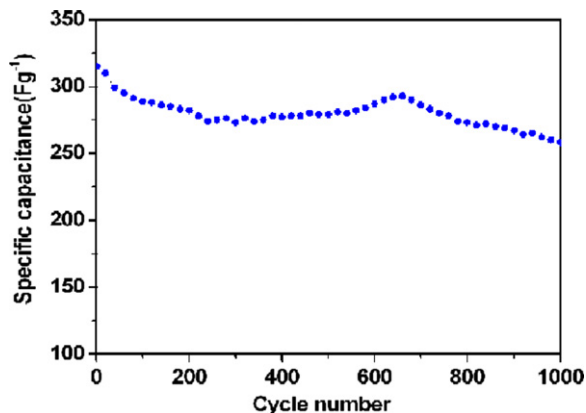| Sample	Specific capacitance/(F g^{-1})		
	100 ± 2/(mA g^{-1})	200 ± 2 (mA g^{-1})	400 ± 2 (mA g^{-1})
FG200	315 ± 5	304 ± 5	287 ± 5
FG550	135 ± 5	116 ± 5	107 ± 5

Fig. 8. Cycle performance of FG200 electrode.

the pseudocapacitance of electrodes decreased accordingly. Thus, the capacitances were obviously lower than FG200.

The charge/discharge efficiency is characterized by the following Eq. (3):

$$\eta = t_{dic}/t_c \tag{3}$$

Where, t_c is charging time, t_{dic} is discharging time. According to Eq. (3), the charge/discharge efficiency of FG200 electrodes was also measured. The maximum charge/discharge efficiency using KOH as electrolyte was about 97% at a current density of 100 mA g^{-1} showed good charge/discharge performance.

The cycle performance of supercapacitors based on FG200 was also investigated by DC at 100 mA g^{-1}. As can be seen from Fig. 8, the initial value was the maximum, but the capacitance of supercapacitors didn't degrade consistently. After 500 cycling, the capacitance increased slightly, contrary to what we might suppose. The abnormal increased capacitive effects might be attributed to the reduction of oxygen-containing functional groups, the fast and reversible Faradic reactions could be the main reason to cause the improvement of capacitance [14], but the details of the impact of the functional groups on electrochemical behaviors still needed further research. However, after 700 cycling, the capacitance started to decrease slightly again. The specific capacitance still retained at a high level with 258 F g^{-1} after 1000 cycles showed great potential application of graphene-based supercapacitors.

4. Conclusions

The multi-layer graphene with flourish oxygen functional groups was obtained using completely oxidized graphite exfoliated

at 200 °C and ambient pressure. The supercapacitors constructed with as-prepared graphene exhibited excellent electrochemical performance. With KOH as the electrolyte, the DC measurements showed a high capacitance of 315 F g^{-1} at the current density of 100 mA g^{-1}. This simple method without any auxiliary conditions, such as high vacuum or under hydrogen environment could provide a promising convenient pathway to achieve a mass production of functionalized graphene. In the mean, the supercapacitor electrodes based on these graphene materials presented a promising application prospect.

Acknowledgement

References

[1] K.S. Novoselov, A.K. Geim, S.V. Morozov, Science 306 (2004) 666–669.
[2] A.K. Geim, K.S. Novoselov, Nat. Mater. 6 (2007) 183–191.
[3] J.C. Slonczewski, P.R. Weiss, Phys. Rev. 109 (1958) 272–279.
[4] P.R. Wallace, Phys. Rev. 71 (1947) 622–634.
[5] A.A. Balandin, S. Ghosh, W.Z. Bao, Nano Lett. 8 (2008) 902–907.
[6] S.V. Morozov, K.S. Novoselov, M.J. Katsnelson, Phys. Rev. Lett. 100 (2008) 016602.
[7] Y.B. Zhang, Y.W. Tan, H.L. Stormer, Nature 438 (2005) 201–204.
[8] K.S. Novoselov, Z. Jiang, Y. Zhang, Science 315 (2007) 1379.
[9] A.K. Geim, Science 324 (2009) 1530–1534.
[10] K.I. Bolotin, K.J. Sikes, Z. Jiang, Solid State Commun. 146 (2008) 351–355.
[11] S. Stankovich, D.A. Dikin, G.H.B. Dommett, Nature 442 (2006) 282–286.
[12] S. Sasha, Dmitriy A. Dikin, Rodney S. Ruoff, Carbon 45 (2007) 1558–1565.
[13] M.D. Stoller, S. Park, Y. Zhu, J. An, R.S. Ruoff, Nano Lett. 8 (2008) 3498–3502.
[14] Y. Chen, X. Zhang, D. Zhang, Carbon 49 (2011) 573–580.
[15] Hannes C. Schniepp, Je-Luen Li, Phys. Chem. B 110 (2006) 8535–8539.
[16] Michael J. McAllister, Je-Luen Li, Chem. Mater. 19 (2007) 4396–4404.
[17] S.R.C. Vivekchand, Chandra Sekhar Rout, K.S. Subbrahmanyam, J. Chem. Sci. 120 (2008) 9–13.
[18] Y. Zhu, Shanthi Murali, Carbon 48 (2010) 2118.
[19] Adarsh Kaniyoor, Tessy Theres Baby, Sundara Ramaprabhu, J. Mater. Chem. 20 (2010) 8467–8469.
[20] W. Lv, D.M. Tang, Yan-Bing He, ACS Nano 3 (2009) 3730–3736.
[21] W.S. Hummers, R.E. Offeman, J. Am. Chem. Soc. 80 (1958) 1339.
[22] F. Tuinsta, J.L. Koenig, J. Chem. Phys. 53 (1970) 1126–1130.
[23] A.C. Ferrari, J.C. Meyer, V. Scardaci, C. Casiraghi, Phys. Rev. Lett. 97 (2006) 187401.
[24] Konstantin N. Kudin, Bulent Ozbas, Hannes C. Schniepp, Nano Lett. 8 (2008) 36–41.
[25] Z.S. Wu, Wencai Ren, J. ACS Nano 3 (2009) 411–417.
[26] J.L. Figueiredo, M.F.R. Pereira, M.M.A. Freitas, Carbon 37 (1999) 1379–1389.